The mysterious spinning cylinder—Rigid-body motion that is full of surprises

David P. Jackson, Julia Huddy, Adam Baldoni, and William Boyes

Citation: American Journal of Physics **87**, 85 (2019); doi: 10.1119/1.5086391
View online: https://doi.org/10.1119/1.5086391
View Table of Contents: https://aapt.scitation.org/toc/ajp/87/2
Published by the American Association of Physics Teachers

The mysterious spinning cylinder—Rigid-body motion that is full of surprises

David P. Jackson,[a] Julia Huddy, Adam Baldoni, and William Boyes
Department of Physics and Astronomy, Dickinson College, Carlisle, Pennsylvania 17013

(Received 29 July 2018; accepted 14 December 2018)

We explore the steady-state rotational motion of a cylinder on a flat horizontal surface from a pedagogical perspective. We show that the cylinder's inclination angle depends on its rotational velocity in a surprisingly subtle manner, including both stable and unstable solutions as well as a forbidden region with no (real) solutions. Moreover, the cylinder's behavior undergoes a qualitative change as the aspect ratio decreases below a critical value. Using a high-speed video, we measure the inclination angle as a function of rotation speed and demonstrate good agreement with the theoretical predictions. All aspects of the analysis are well within the capabilities of undergraduate students, making this an ideal system to explore in courses or as an independent project.
https://doi.org/10.1119/1.5086391

I. INTRODUCTION

Rigid-body motion is a standard topic in a classical mechanics course, yet it's one that often leaves students confused. Part of the difficulty lies in the fact that students must simultaneously deal with forces, torques, angular momentum, non-inertial reference frames, the inertia tensor, principal axes, and Euler angles. While none of these topics are particularly difficult by themselves, a rigid-body motion problem can involve all of them and it can be quite challenging for students to keep everything straight, particularly when many of these topics are new. In situations like this, it is not uncommon for students to start blindly following the mathematics, losing all insight into what is going on physically. One way to combat this tendency is to provide students with a real physical example that is captivating yet straightforward to understand. By giving students something they can play around with, they can focus more of their attention on the physics and hopefully use the mathematics as a tool for their exploration.

Two interesting toys that can be used to motivate the study of rigid-body motion are a tippe top,[1,2] which flips itself over, and a rattleback,[3,4] which reverses its direction of spin. Unfortunately, while these toys are certainly captivating, understanding their behavior can be a challenge for undergraduates. Indeed, even the traditional spinning top can be difficult to analyze except under specific conditions, and these conditions do not often materialize when spinning a real top on a table.

One toy that is both alluring and straightforward to understand goes by the name of *Hurricane Balls*. This toy, discussed in the literature not long ago,[5] makes a great addition to a classical mechanics course and can be used as a demonstration or as an extended homework problem or student project.[6] One of the reasons this toy is so effective at engaging students is its simplicity—Hurricane Balls consists of nothing more than two steel balls that have been glued (or welded) together. It is very easy to get Hurricane Balls spinning and the resulting motion is clearly non-trivial while being perfectly reproducible, allowing for both theoretical and experimental investigations. Furthermore, a compressed air source can be used to get Hurricane Balls spinning so fast ($\sim$100 Hz) that the centrifugal forces will rip the balls apart (assuming they are glued together), which is always exciting to students.

Here, we report on a similar toy that consists of nothing more than a short cylindrical tube made of polyvinyl chloride (PVC). Such a tube can be set spinning by laying it down on a flat table, placing a finger on top of one end, and then pushing down fairly hard until the end of the cylinder shoots out from under the finger, with the finger snapping down onto the table. Although the motion of the spinning cylinder is itself somewhat captivating, the real surprise comes when the ends of the cylinder are labelled with an X and an O, as shown in Fig. 1. Surprisingly, if one pushes down on the X to get the cylinder spinning, one will see only Xs when viewed from above. Similarly, if one pushes down on the O, then only Os will be visible (see Fig. 1). The fact that one of the letters disappears from sight when the cylinder is spun is quite surprising to students, and this mystery can provide powerful motivation to try to understand what is happening. In fact, before reading further, I encourage you to go find such a cylinder and try to figure out the mystery for yourself.

It is not clear when this mysterious phenomenon was first discovered. Mamola,[7] who provides a fairly detailed discussion of the basic physics, reports seeing this device presented at an AAPT meeting in 1993. More recently, the pedagogical benefits of this surprising effect were promoted as an authentic laboratory experience for undergraduate students,[8] with one of the authors stating that they had seen this device at a regional AAPT meeting "around 1990." However, due to the simplicity of the system involved, it is likely that this phenomenon has been "discovered" many times prior to 1990. Indeed, a fairly thorough investigation of the spinning cylinder's motion was carried out in the early 1980s by Whitehead and Curzon,[9] though there is no mention of the mysterious disappearing-symbol behavior described above (this work was also the impetus for a beautifully written essay for *The Amateur Scientist* column in Scientific American[10]).

The spinning-cylinder mystery has been widely discussed on the internet, perhaps most prominently on the *Veritasium* YouTube channel, where it has been viewed nearly four million times.[11] Such a large number of views demonstrates that this phenomenon is inherently interesting to the general public and is one reason why this system is ideally suited to help motivate students in class.

Although the spinning-cylinder problem has a relatively short publication history, the closely related problem of a

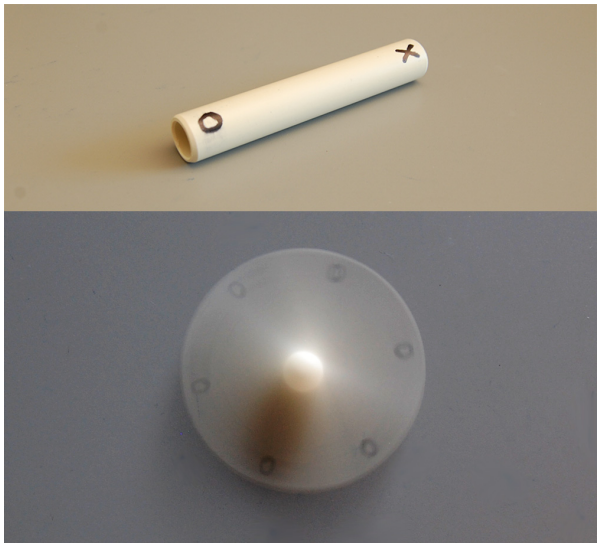

Fig. 1. Top: A piece of $\frac{5}{8}$-in. diameter PVC pipe with a length of $3\frac{3}{4}$ inches has an X and an O marked on the ends. Bottom: A photograph of this tube after being spun by pushing down on the O and launching the cylinder by snapping the finger down. Note that there are six Os visible but none of the Xs can be seen. This surprising behavior provides good motivation when students are learning about rigid-body motion (enhanced online).

disk rolling on a horizontal surface has been extensively discussed in the literature. According to Shegelski *et al.*,[12] this problem was first studied by Poisson as far back as 1883 and has since been studied by many authors (Ref. 12 provides a brief but reasonably complete history). A coin rolling on a table is something that will be familiar to all students; however, solving the problem in general turns out to be surprisingly complex.[13] As such, several authors have analyzed special cases of the motion in order to simplify the mathematics and make the problem more accessible to students.[14–16]

Renewed interest in the rolling disk problem came as a result of a commercially available toy called *Euler's Disk*.[17] Like the mysterious spinning cylinder, Euler's Disk is quite captivating and makes an excellent demonstration in a classical mechanics course.[18] The toy consists of a thick metal disk that is spun like a coin on a smooth (slightly concave) surface. After some time, the disk will begin rolling on its rim, and as the disk gets closer to being horizontal, the rotation frequency can be heard to increase quite dramatically. The entire process takes several minutes to complete, but it is what happens right near the end that is of current interest. This behavior has been described by Moffat[19] as a "finite-time singularity"; in his words, the disk ultimately "comes to rest quite abruptly, the final stage of motion being characterized by a shudder and a whirring sound of rapidly increasing frequency." Immediately after Moffat's analysis appeared, a debate ensued as to precisely what is responsible for the energy loss in this system.[20] Research on various aspects of Euler's Disk continues to this day, although it now appears clear that the dominant energy-loss mechanism near the end of the motion is due to rolling friction.[21]

In this article, we investigate a spinning cylinder in a manner that is appropriate for use with sophomore or junior students. Our treatment is designed to be pedagogical in nature so the presentation includes topics such as vector analysis, rotation matrices, the inertia tensor, and principal axes. Our study is limited to the steady-state motion of the cylinder in which the center of mass remains at rest. Despite this restriction, the theoretical analysis turns out to be remarkably rich and leads to a number of surprising results. We also present experimental data obtained from the high-speed video that show good agreement with the theory.

II. THEORY

A. Qualitative analysis

Before embarking on a full mathematical treatment, it is helpful to give each student their own cylinder so that they can play around and make some qualitative observations.[22] They should be encouraged to try different things such as spinning the cylinder faster or slower or viewing the spinning cylinder from different angles. Two things should soon become clear: (i) if the cylinder is not launched fast enough, it never really gets going and the disappearing-symbol phenomenon is not observed, and (ii) if spun fast enough, there is a brief transient period where the motion is quite complex, but the cylinder quickly settles into a fairly simple steady-state motion. If we focus our attention on this steady-state motion, the following observations can be made:

- The center of mass is nearly at rest (it moves downward, but it does so very slowly).
- The cylinder is not spinning flat on the table; instead, one end is up in the air.
- The faster the cylinder is spun the more it "stands up" on end; however, it appears that the cylinder will not rise above some maximum angle with the table.
- The cylinder rolls without slipping on the table.

The rolling-without-slipping constraint is one that students might not notice on their own. This constraint can be understood by analogy with a hula-hoop rolling along the floor. Imagine a hula-hoop of radius R spun on the floor with a large angular velocity ω and no linear velocity ($v=0$). The hula-hoop initially slides against the floor, resulting in a (kinetic) frictional force that acts to decrease the angular velocity while simultaneously increasing the linear velocity. As long as the hula-hoop continues to slide against the floor, the kinetic frictional force will continue to act. The result is that the angular velocity continues decreasing and the linear velocity continues increasing until the rolling condition $v=\omega R$ is met. At this point, the hula-hoop rolls without slipping and will continue to do so until rolling friction (and air resistance) brings it to a stop.

After making these qualitative observations, it is helpful to show a slow-motion movie to give students a better look at the cylinder's motion. We have included such a movie as supplementary material to this article.[23] Besides demonstrating that the cylinder really does roll without slipping, the movie also clearly shows that both the X and the O face up at the same time (as, of course, must be the case).

In order to analyze this system, we will make only a single simplification: we will assume that during the steady-state motion, the center of mass remains at rest. At first glance, it might appear that this assumption is so drastic as to render the problem trivial, but it turns out that there is still much to learn. Recall that our goal here is not to solve the spinning cylinder problem in general. Instead, we want to help students learn how to analyze a complex real-world problem and gain as much physical insight as possible. Note that by assuming a stationary center of mass, we are implicitly assuming that the cylinder maintains a fixed angle with the

table and that it spins at a constant rate (i.e., no energy is lost from the system so that friction and air drag are assumed to be negligible).

B. Fundamental equations

A natural starting point is Newton's second law of motion

$$\mathbf{F}_{\text{net}} = m\mathbf{a}. \tag{1}$$

Here, m is the mass of the cylinder and $\mathbf{a}$ is the acceleration of the center of mass. Because we are neglecting both frictional forces and air resistance, there are only two forces acting on the cylinder: the gravitational force acting downward through the center of mass and the normal force $\mathbf{F}_N$ of the table on the cylinder acting upward at the point of contact. If the center of mass remains fixed, the net force will be zero, giving

$$\mathbf{F}_N = -m\mathbf{g}, \tag{2}$$

where $\mathbf{g}$ is the gravitational field. Thus, we see that the normal force has a magnitude equal to the gravitational force and points in the opposite direction, something we probably could have guessed at the outset. Unfortunately, there is nothing else to learn from Newton's second law.

The reason Newton's second law is not very helpful is because the motion is purely rotational, and although the net force is equal to zero, there is a nonzero net torque acting on the system. In order to make progress, therefore, we need to invoke the rotational version of Newton's second law, namely,

$$\boldsymbol{\Gamma}_{\text{net}} = \frac{d\mathbf{L}}{dt}. \tag{3}$$

Here, $\boldsymbol{\Gamma}_{\text{net}}$ represents the net torque about the center of mass and $\mathbf{L}$ is the angular momentum of the cylinder.[24]

Before moving forward, we need a sketch that shows the geometry of the situation and defines an appropriate coordinate system. While any coordinate system can be used, some are more useful than others and students should be advised to take advantage of the symmetry of the cylinder. Figure 2 shows a sketch of the cylinder at one instant of time (say, $t = 0$) and includes two different coordinate systems, both

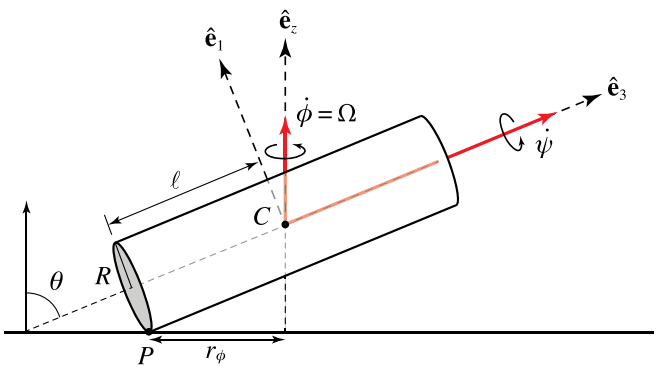

Fig. 2. The geometry of the spinning cylinder (both $\hat{\mathbf{e}}_y$ and $\hat{\mathbf{e}}_2$ point out of the page). A cylinder of mass M, half-length ℓ, and radius R rolls without slipping on a horizontal surface. The (x, y, z) coordinate system is an inertial (laboratory) system that remains fixed, while the (1, 2, 3) system rotates about the vertical axis with angular speed $\dot{\phi}$ (and thus remains aligned with the cylinder).

with their origins at the cylinder's center of mass C. The (x, y, z) system is an inertial laboratory coordinate system that does not change with time, while the (1, 2, 3) system is a (non-inertial) set of principal axes that maintains its alignment with the object, rotating about the vertical. We include two coordinate systems because (i) Eq. (3) is only valid in an inertial coordinate system and (ii) we want to take advantage of the symmetry of the cylinder. Both of these coordinate systems will prove useful in the analysis.[25]

It is important to note that the (1, 2, 3) non-inertial coordinate system is *not* a "body-fixed" coordinate system, as is usually adopted in such a situation. Although our choice here is somewhat non-standard, the use of such a coordinate system simplifies the analysis by eliminating any dependencies on ψ (see Fig. 2).

C. The angular velocity vector

The cylinder in Fig. 2 has mass M, half-length ℓ, and radius R, while the angles θ, ϕ, and ψ (the so-called Euler angles) specify its orientation in space (with $0 \le \theta \le \pi/2$ in this case). Because we are assuming that the center of mass remains fixed, the angle θ will be constant. Likewise, the rotational velocities $\dot{\phi}$ (about the vertical axis) and $\dot{\psi}$ (about the symmetry axis) will also be constant. In terms of these angles, the angular velocity is most simply written as

$$\boldsymbol{\omega} = \dot{\phi}\,\hat{\mathbf{e}}_z + \dot{\psi}\,\hat{\mathbf{e}}_3. \tag{4}$$

To take advantage of the symmetry of the cylinder, the angular velocity can be expressed solely in terms of the principal axes as

$$\boldsymbol{\omega} = \dot{\phi}\sin\theta\,\hat{\mathbf{e}}_1 + (\dot{\phi}\cos\theta + \dot{\psi})\,\hat{\mathbf{e}}_3. \tag{5}$$

To proceed further, we need to determine the relationship between $\dot{\phi}$ and $\dot{\psi}$, which can be found from the geometry of Fig. 2. Because the cylinder rolls without slipping, the point of contact P traces out a circle of radius r_ϕ on the table while simultaneously tracing out a circle of radius R on the cylinder. Thus, the velocity of the point of contact will be the same on the table and the cylinder so that $v_\phi = r_\phi\dot{\phi} = v_\psi = R\dot{\psi}$. From the geometry of Fig. 2, we find that $r_\phi = \ell\sin\theta - R\cos\theta$, giving

$$\dot{\psi} = (\tilde{\ell}\sin\theta - \cos\theta)\dot{\phi}, \tag{6}$$

where $\tilde{\ell} = \ell/R$ is the (dimensionless) aspect ratio of the cylinder. In our analysis, we will assume that $\dot{\phi} > 0$. However, note that as written r_ϕ can be positive or negative depending on whether the point of contact P lies to the left or right, respectively, of the center of mass C. The result is that $\dot{\psi}$ can be positive or negative (or zero) depending on the value of θ. We will return to this point later, but for the situation shown in Fig. 2, we note that $\dot{\psi} > 0$. Then, defining $\Omega \equiv \dot{\phi}$ (>0) and substituting into Eq. (5), we find

$$\boldsymbol{\omega} = \Omega\sin\theta(\hat{\mathbf{e}}_1 + \tilde{\ell}\,\hat{\mathbf{e}}_3), \tag{7}$$

which gives the instantaneous angular velocity of the cylinder.

In order to gain some insight into what Eq. (7) is telling us, notice that both components of the angular velocity have

the same θ-dependence. Thus, the angle γ that $\boldsymbol{\omega}$ makes with the symmetry axis is independent of θ (see Fig. 3):

$$\gamma = \arctan\left(\frac{\omega_1}{\omega_3}\right) = \arctan\left(\frac{R}{\ell}\right). \tag{8}$$

In other words, the angular velocity vector always points along the vector $\mathbf{r}_+ = R\,\hat{\mathbf{e}}_1 + \ell\,\hat{\mathbf{e}}_3$ and thus passes through the uppermost point on the cylinder (point O in Fig. 3). The instantaneous axis of rotation therefore consists of a line through the diagonal of the cylinder that passes through the point of contact P, the center of mass C, and the uppermost point O.

At this point, some students may have figured out why only one symbol is visible when the cylinder is spun (though most, probably, will have not). To make things somewhat more explicit, students can be asked to calculate the (linear) velocity at locations $\mathbf{r}_\pm = R\,\hat{\mathbf{e}}_1 \pm \ell\,\hat{\mathbf{e}}_3$ on the cylinder (points O and X in Fig. 3). By calculating $\mathbf{v}_\pm = \boldsymbol{\omega} \times \mathbf{r}_\pm$, one will see that two velocities come into play, one due to rotation about the 1-axis and the other due to spin about the 3-axis, and that these two velocities have exactly the same magnitude. At location $\mathbf{r}_+$, these velocities are in opposite directions and will exactly cancel; at location $\mathbf{r}_-$, they are in the same direction and will add together. The net result is that when viewed from above, one end of the cylinder (point O in Fig. 3) will be instantaneously at rest while the other end (point X) will be moving quite rapidly.[26,27]

It is worth mentioning that a highly motivated student can figure all of this out qualitatively just by playing around with a cylinder and thinking about the motion. It is not too difficult to see that when you launch the cylinder with your finger, one end moves away from you while the other end moves toward you. At the same time, your finger imparts "backspin" to the cylinder, which gives the top of the cylinder a velocity toward you (on both ends).[28]

D. The angular momentum vector

Next, we turn our attention to the angular momentum vector $\mathbf{L}$. A student's first inclination might be to use the equation $\mathbf{L} = I\boldsymbol{\omega}$, with I being the moment of inertia; however, this equation assumes that both $\mathbf{L}$ and $\boldsymbol{\omega}$ point in the same direction, which is not the case here. Instead, we must use

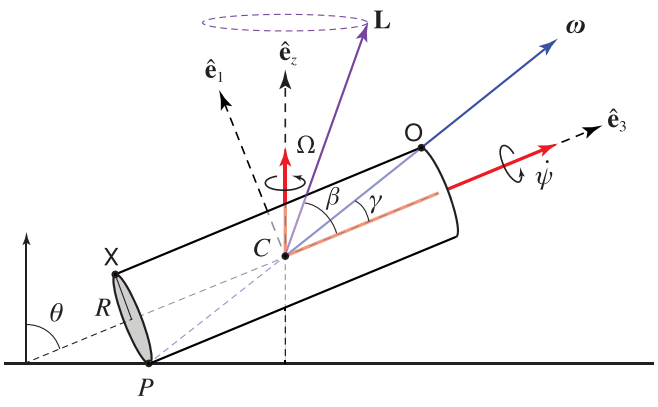

Fig. 3. The angular velocity vector $\boldsymbol{\omega}$ always passes through the uppermost point O on the cylinder, independent of the angle θ. For the situation shown here (corresponding to $I_1 > I_3$), the angular momentum vector lies further from the symmetry axis compared to $\boldsymbol{\omega}$ (i.e., $\beta > \gamma$).

the more general version of this equation $\mathbf{L} = \mathbb{I} \cdot \boldsymbol{\omega}$, where $\mathbb{I}$ here is the inertia tensor. If tensors are new to the students, some discussion will inevitably be required to get them familiar with the concept.

As with a vector, the components of $\mathbb{I}$ will depend on the coordinate system used, so it is now more important than ever to choose a coordinate system carefully. The (1, 2, 3) coordinate system in Fig. 2 is composed of a set of principal axes in which the inertia tensor is diagonal; this simplifies the problem considerably.[29] The diagonal elements of the inertia tensor are the moments of inertia about the three principal axes, which we write as I_1, I_2, and I_3. In this coordinate system, the angular momentum vector is then $\mathbf{L} = I_1\omega_1\,\hat{\mathbf{e}}_1 + I_2\omega_2\,\hat{\mathbf{e}}_2 + I_3\omega_3\,\hat{\mathbf{e}}_3$, and using Eq. (7) we find that

$$\mathbf{L} = \Omega \sin\theta (I_1\,\hat{\mathbf{e}}_1 + I_3\tilde{\ell}\,\hat{\mathbf{e}}_3). \tag{9}$$

Just like with the angular velocity vector $\boldsymbol{\omega}$, we see that both components of the angular momentum vector have exactly the same dependence on θ. We therefore find that the angle β that $\mathbf{L}$ makes with the symmetry axis is independent of θ (see Fig. 3):

$$\beta = \arctan\left(\frac{L_1}{L_3}\right) = \arctan\left(\frac{I_1}{I_3}\frac{R}{\ell}\right). \tag{10}$$

Referring to Eq. (8), we see that when $I_1 = I_3$, the angles γ and β will be equal. In this case, $\mathbf{L}$ will be proportional to $\boldsymbol{\omega}$ and the introductory physics formula $\mathbf{L} = I\boldsymbol{\omega}$ will indeed be valid. For the situation shown in Fig. 3, where $I_1 > I_3$ (which we take to define a "cylinder"[31]), Eqs. (8) and (10) lead to $\beta > \gamma$. Similarly, when $I_1 < I_3$ (a "disk"), we find that $\beta < \gamma$. The vector $\mathbf{L}$ is sketched in Fig. 3 and is observed to precess about the vertical axis at a constant rate Ω (along with the cylinder and all other vectors in this figure). The precession of $\mathbf{L}$ is a result of there being a net torque about the center of mass. Students can readily verify using the right-hand rule that this torque acts in the negative y direction (into the page in Fig. 3), as expected from the direction of precession ($d\mathbf{L}$ also points into the page).

The stage is now set to explicitly calculate the torque and apply Eq. (3). Before doing so, however, we discuss a subtle and interesting feature of Fig. 3.

Recall that one of our qualitative observations was that the faster the cylinder is spun the more it "stands up." Mathematically, this means that the angle θ decreases as the rotation rate Ω increases. But it was also noticed that there appears to be a limit to how much the cylinder will stand up, which suggests that there may be a minimum value (θ_{min}) to θ. Looking at Fig. 3, we see that as θ decreases, the component of $\mathbf{L}$ perpendicular to the vertical ($L_\perp$)—the portion of $\mathbf{L}$ that changes with time—becomes smaller. In fact, as $\theta \to \beta$, we see that $L_\perp \to 0$. But when $\theta = \beta$, there will still be a finite torque in the negative y direction. Therefore, the only way to keep $d\mathbf{L}/dt$ finite as $\theta \to \beta$ (so that it balances the applied torque) is for the rotation rate to increase without bound. In other words, $\Omega \to \infty$ as θ approaches will approach the value $\beta = \arctan(I_1 R/I_3\ell)$. Note that without even solving the equation of motion, we have arrived at a concrete prediction based solely on physical grounds. Such arguments are well worth discussing with students before embarking on a full mathematical treatment of the problem.

E. The equation of motion

At this point, one might be tempted to use Eq. (7) to write the kinetic energy of the system as $T = \frac{1}{2}(I_1\omega_1^2 + I_3\omega_3^2)$ and use a Lagrangian approach to solve this problem. However, unlike the situation with Hurricane Balls,[6] such an approach will fail here due to the rolling-without-slipping constraint being nonholonomic.[30] Fortunately, using Eq. (3) is quite straightforward. The only force that causes a torque about the center of mass is the normal force $\mathbf{F}_N$, which gives

$$\begin{aligned}\boldsymbol{\Gamma}_{\text{net}} &= \mathbf{r} \times \mathbf{F}_N = (-R\,\hat{\mathbf{e}}_1 - \ell\,\hat{\mathbf{e}}_3) \times Mg\,\hat{\mathbf{e}}_z \\ &= MgR\cos\theta(1 - \tilde{\ell}\tan\theta)\hat{\mathbf{e}}_2. \end{aligned} \tag{11}$$

In principle, we need to equate this torque to the time derivative of the angular momentum vector in Eq. (9). However, there is no obvious time dependence in Eq. (9), so students might be tempted to say that $d\mathbf{L}/dt$ is equal to zero. The problem is that Eqs. (9) and (11) are written in terms of the non-inertial (1, 2, 3) coordinate system, whereas Eq. (3) is only valid in an inertial reference frame. In other words, there is an implicit time-dependence to the basis vectors $\hat{\mathbf{e}}_1$, $\hat{\mathbf{e}}_2$, and $\hat{\mathbf{e}}_3$ (recall that Fig. 2 is drawn at time $t = 0$). To proceed further, therefore, we need to explicitly add in the time dependence to Eqs. (9) and (11). Because the vectors $\mathbf{L}$ and $\boldsymbol{\Gamma}$ precess about the z-axis at a constant rate Ω, an instructive way to incorporate this time dependence is to use rotation matrices.

The matrix

$$\mathsf{R}_z(\xi) = \begin{pmatrix} \cos\xi & -\sin\xi & 0 \\ \sin\xi & \cos\xi & 0 \\ 0 & 0 & 1 \end{pmatrix} \tag{12}$$

is the (*active*) rotation matrix for a rotation about the z-axis. Specifically, when applied to a column vector consisting of (x, y, z) components, that vector is seen to rotate about the z-axis by an angle ξ. Applying the (time-dependent) matrix $\mathsf{R}_z(\Omega t)$ would then lead to a vector that rotates about the z-axis with a constant angular velocity Ω, precisely what we want the vectors $\mathbf{L}$ and $\boldsymbol{\Gamma}$ to do. Thus, to make the time dependence explicit in Eqs. (9) and (11), we merely need to write these vectors in terms of their (x, y, z) components and apply the matrix $\mathsf{R}_z(\Omega t)$.

Let us begin with the torque vector in Eq. (11). At $t = 0$, Fig. 2 shows that $\hat{\mathbf{e}}_2 = \hat{\mathbf{e}}_y$. Therefore, the torque at $t = 0$ is given by $\boldsymbol{\Gamma}(0) = MgR\cos\theta(1 - \tilde{\ell}\tan\theta)\hat{\mathbf{e}}_y$. Applying the (time-dependent) rotation matrix to this vector then gives

$$\begin{aligned}\boldsymbol{\Gamma}(t) &= \mathsf{R}_z(\Omega t)\boldsymbol{\Gamma}(0) \\ &= -MgR\cos\theta(1 - \tilde{\ell}\tan\theta)\left[\sin(\Omega t)\,\hat{\mathbf{e}}_x - \cos(\Omega t)\,\hat{\mathbf{e}}_y\right]. \end{aligned} \tag{13}$$

For the angular momentum vector in Eq. (9), we must first break $\hat{\mathbf{e}}_1$ and $\hat{\mathbf{e}}_3$ into their x and z components before applying the rotation matrix; the end result is

$$\begin{aligned}\mathbf{L}(t) = I_3\Omega\sin\theta\cos\theta\{&(I_1/I_3 - \tilde{\ell}\tan\theta) \\ &\times \left[\cos(\Omega t)\,\hat{\mathbf{e}}_x - \sin(\Omega t)\,\hat{\mathbf{e}}_y\right] + (I_1/I_3 - \tilde{\ell})\hat{\mathbf{e}}_z\}. \end{aligned} \tag{14}$$

As expected, L_z has no time-dependence—any vector that rotates about the z-axis will have a constant z-component. The equation of motion is finally found by taking the time derivative of Eq. (14) and equating it to Eq. (13), giving

$$\tilde{\Omega} = \sqrt{\frac{1 - \tilde{\ell}\tan\theta}{(I_1/I_3 - \tilde{\ell}\tan\theta)\sin\theta}}, \tag{15}$$

where $\tilde{\Omega} \equiv \Omega/\sqrt{MgR/I_3}$ is a dimensionless rotation rate.

III. ANALYSIS OF THE EQUATION OF MOTION

Equation (15) contains a tremendous amount of information and analyzing it can be somewhat intimidating for students. In such a situation, it can be helpful to begin by examining some limiting cases.

A. Limiting cases

One limiting case occurs when the rotation speed goes to zero, which happens when the numerator in Eq. (15) goes to zero, or when $\theta = \theta_0 \equiv \arctan(R/\ell)$. This angle is one we have seen before [see Eq. (8)] and represents the angle γ between $\boldsymbol{\omega}$ and the symmetry axis. From Fig. 3, we see that when $\theta = \gamma$, the angular velocity points along the vertical, so the center of mass lies directly above the point of contact. In other words, the rotation rate is zero when the cylinder is balanced on a single point. Although this is a valid solution to Eq. (15), it is clearly an unstable situation and not one that is likely to be observed experimentally.

Another limiting case is when the rotational speed goes to infinity. This situation was briefly discussed in Sec. II D on purely physical grounds. Here, we look at the situation mathematically by letting the denominator in Eq. (15) go to zero. We find two possibilities: either $\theta \to \theta_\infty \equiv \arctan(I_1R/I_3\ell)$ or $\theta \to 0$. As already discussed, the angle θ_∞ $(=\beta)$ occurs when the angular momentum vector points along the vertical axis [see Eq. (10) and Fig. 3], so this solution is to be expected. On the other hand, the solution $\theta \to 0$ corresponds to the cylinder oriented so that it stands vertically on one of its ends. This solution may come as a bit of a surprise to students.[32] One can picture this situation as the "wobbling" motion of an empty bottle or can that has been gently spun while standing nearly upright.

One final limiting case we can examine is when $\theta \to \pi/2$. This situation corresponds to the cylinder lying on its side, with one end just beginning to lose contact with the table. Taking the appropriate limit in Eq. (15) leads to $\tilde{\Omega} \to 1$ and corresponds to the critical rotation rate $\Omega_c = \sqrt{MgR/I_3}$ necessary to achieve the steady-state motion depicted in Fig. 2. Interestingly, a cylindrical tube has moment of inertia $\approx MR^2$ about the symmetry axis so that $\Omega_c = \sqrt{g/R}$ is independent of both ℓ and M. For the piece of PVC pipe shown in Fig. 1, an order-of-magnitude estimate gives $\Omega_c \approx \sqrt{(10\text{ m/s}^2)/(10^{-2}\text{ m})} \approx 32\text{ rad/s} \approx 5\text{ Hz}$. Playing around with this cylinder shows that this value seems just about right.

B. Detailed analysis

Now that we have looked at the limiting cases, let us explore the complete set of solutions to Eq. (15) in more detail. We found it convenient to use solid cylinders (and

disks) for our experiments, so we will adopt $I_3 = \frac{1}{2}MR^2$ and $I_1 = \frac{1}{2}MR^2[\frac{1}{2}(1 + 4\tilde{\ell}^2/3)]$ for the remainder of this paper.

The solutions to Eq. (15) will only be real when the quantity under the radical is positive. Therefore, both the numerator and the denominator must be either positive or negative. Having just determined when the numerator and denominator are equal to zero (at θ_0 and θ_∞, respectively), it is straightforward to confirm that there will only be real solutions when $\theta > \theta_0, \theta_\infty$ or when $\theta < \theta_0, \theta_\infty$. In other words, there will be no real solutions when θ lies between θ_0 and θ_∞. This information is displayed in Fig. 4, where we plot both θ_0 and θ_∞ as a function of the aspect ratio $\tilde{\ell}$. Note the "forbidden" regions (dark gray) where there are no real solutions to Eq. (15). Each point outside these regions represents a valid steady-state solution.

Some of the features of Fig. 4 have been previously discussed.[9,10] The curves θ_∞ and θ_0 represent boundaries between the forbidden regions and regions where real solutions exist. These curves cross at an aspect ratio of $\tilde{\ell} = \sqrt{3}/2$ (vertical dashed line), which leads to different behaviors to the right and left of this value. This aspect ratio corresponds to the point where $I_1 = I_3$ and marks the dividing line between "cylinders" ($\tilde{\ell} > \sqrt{3}/2$) and "disks" ($\tilde{\ell} < \sqrt{3}/2$). The areas above and below the forbidden regions correspond to different types of motion: the upper region represents cylinders spinning on their sides (or disks spinning on their edges) and having $\psi > 0$ [see Eq. (6)]; the lower region represents cylinders spinning on their ends (or disks spinning on their faces) and having $\psi < 0$.

One feature of Fig. 4 that has not been previously discussed is the stability of the solutions. As discussed earlier, the solutions along the curve θ_0 represent the cylinder (or disk) balancing on a single point of contact with $\tilde{\Omega} = 0$. Such solutions are obviously unstable. In fact, there is a band of unstable solutions adjacent to this curve, depicted by light gray shading and bounded by the dashed multi-valued curve. (The details of the stability calculation are presented in the Appendix so as not to interrupt the flow of the discussion.) Thus, a cylinder spinning on its end (lower right portion of Fig. 4) will be unstable once θ becomes too large. Similarly, disks spinning on their sides are only stable for relatively large aspect ratios ($\tilde{\ell} \gtrapprox 0.477$) and for large angles ($\theta$ near $\pi/2$). Interestingly, there is a small range of aspect ratios

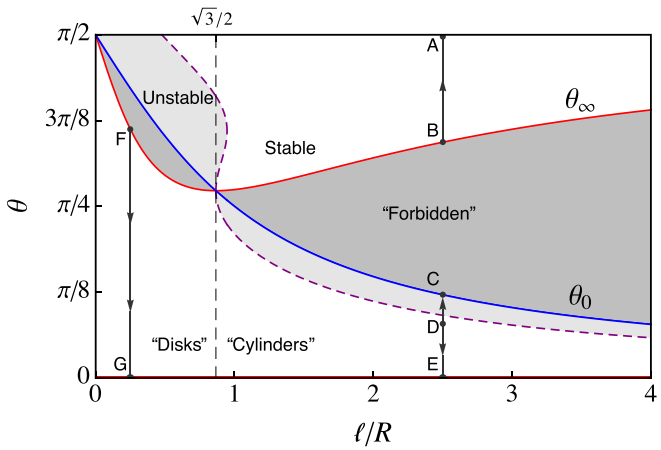

Fig. 4. A θ-$\tilde{\ell}$ phase portrait for the steady-state solutions of the spinning cylinder, Eq. (15), showing both stable and unstable solutions, as well as a forbidden region in which there are no (real) solutions.

(between $\sqrt{3}/2$ and ≈ 0.9465) in which there are two stable regions separated by an unstable region for cylinders spinning on their sides. Again, we note that even though these unstable motions represent valid solutions to Eq. (15), it is not expected that they would be observable experimentally.

Figure 4 contains a lot of information and can be a bit overwhelming for students to comprehend, at least initially. One way to clarify what is going on is to consider a specific aspect ratio and imagine what happens as $\tilde{\Omega}$ (or θ) is varied. For example, consider an aspect ratio of $\tilde{\ell} = 2.5$ and imagine spinning the cylinder while on its side so that we are in the upper portion of the graph. Recall that sustained steady-state motion is not possible unless the cylinder is spun with $\tilde{\Omega} \geq 1$, in which case the cylinder would just be entering the steady-state regime at $\theta = \pi/2$ (point A on the graph). As we increase the angular speed, perhaps by using an air source, the angle θ decreases (as the cylinder stands up) and we move vertically down on the graph. As we continue increasing the angular speed, we move further down vertically (more and more slowly), approaching the curve θ_∞ as $\tilde{\Omega} \to \infty$ (point B). At this point, we reach the forbidden region and θ will not decrease any further. In this sense, the curve θ_∞ represents a minimum angle for cylinders spinning on their sides.

As we increase $\tilde{\Omega}$ as just described, the energy of the system is seen to increase as well. Although our analysis assumed that there were no energy losses in the system, there will always be dissipation in any real system. Thus, if one spins up a cylinder in a real experiment and lets it evolve naturally, the rotation speed will decrease as the system loses energy, causing θ to increase. This behavior is indicated by the arrow on the vertical line adjoining points A and B, depicting the "downhill" flow of energy in the system.

Now consider point C on the graph. Here, the angular speed is $\tilde{\Omega} = 0$ and the cylinder is balanced with its center of mass directly above the point of contact. Moving down vertically, θ will again decrease as $\tilde{\Omega}$ (and the energy) increases. The steady-state motion thus consists of a slowly rotating cylinder that is very near the balancing angle. This too is an unstable solution. As θ decreases further (and $\tilde{\Omega}$ continues increasing), we will eventually reach a point where the motion becomes stable (we have crossed the dashed curve). For a small range of angles below this point, the energy will continue to rise. Thus, if a real cylinder (subject to friction and air resistance) is spinning in this range of angles, the system will evolve upwards (θ will *increase*) on the graph as the energy flows downhill. In other words, the stable motion will be "pulled" into the unstable region. However, as θ decreases further, we soon reach an angle (point D, $\theta \approx 0.25$) where the energy of the system begins decreasing.[33] A real spinning cylinder with angles below this value will evolve so that θ *decreases*, with $\tilde{\Omega}$ increasing (to ∞) as $\theta \to 0$ (point E).

One can analyze the motion of disks in a similar manner. For example, a disk with aspect ratio $\tilde{\ell} = 0.25$ (similar to *Euler's Disk*) has no stable motions for spinning on its edge. The first stable motion occurs when the disk is spinning on its face with $\theta \to \theta_\infty$ and $\tilde{\Omega} \to \infty$ (point F in Fig. 4). As θ decreases initially, both the rotation rate and the system energy will decrease. However, as θ decreases further, we soon reach a point where the rotation rate begins increasing even though the energy continues to decrease. This behavior continues until $\theta \to 0$ and $\tilde{\Omega}$ again approaches ∞ (point G). This motion will probably be familiar to most students—a

coin spinning rapidly on a table undergoes the exact motion just described, ending with an impressive increase in the rotation rate Ω just before coming to rest flat on the table (essentially a miniature version of *Euler's Disk*).[34]

Finally, it is worth noting that there is no forbidden region for the specific aspect ratio $\tilde{\ell} = \sqrt{3}/2$. Lying right at the boundary between disks and cylinders, this aspect ratio contains solutions (not all stable) for the entire range of angles $0 < \theta < \pi/2$. Interestingly, the two curves θ_0 and θ_∞ cross at $\tilde{\ell} = \sqrt{3}/2$, suggesting that the angle $\theta = \arctan(R/\ell)$ supports solutions for both $\tilde{\Omega} = 0$ and $\tilde{\Omega} = \infty$. This situation is discussed in more detail in the following section.

IV. EXPERIMENTAL RESULTS

So far, our analysis has been completely theoretical. One of the nice aspects of this particular system is that it is relatively easy to construct cylinders with different aspect ratios and perform experiments. Unfortunately, unlike *Hurricane Balls*, which lead to extremely stable and reproducible experimental results, it is a bit more difficult to obtain experimental data for spinning cylinders and disks. The main issue is that the system is much more prone to instabilities that are not accounted for in our theory. For example, a cylinder with aspect ratio $\tilde{\ell} = 1$ is quite stable when spinning extremely fast. However, as the rotation rate $\tilde{\Omega}$ decreases, the center of mass of the system will suddenly begin circling around in a fairly predictable manner. While this motion and the underlying instability are quite interesting and would make a nice extension to the analysis presented here, such motions are beyond the scope of this study. Nevertheless, because of such instabilities, it is important when taking experimental data to be as careful as possible that the motion is actually one in which the center of mass is (nearly) at rest and the angle θ is (nearly) constant.[35]

The easiest experimental data to obtain are when the cylinders (or disks) are spinning extremely fast, as the steady-state motion is very stable at high rotation rates. In addition, Eq. (15) leads to the specific prediction $\theta_\infty = \arctan(I_1/I_3\tilde{\ell})$ for this situation. Using an air source and two handheld nozzles, it is relatively easy to drive the system to very high rotation rates (typically $\gtrsim 100$ Hz). A high-speed camera is then used to capture the motion from which data are obtained using the freely available video-analysis program *Tracker*.[36] Figure 5 shows a sample of our results for a range of different aspect ratios (the error bars are approximately the size of the markers). As can be seen, these data agree with the prediction quite well, though there appears to be a small systematic error for larger aspect ratios. This effect can be understood by noting that smaller-aspect-ratio cylinders level off to θ_∞ more quickly and will therefore be better approximated by finite rotation rates (see Fig. 6).

To obtain data for different rotation rates, we would spin a cylinder up to a high rotation rate and then make short videos as energy is dissipated and the rotation rate decreases. Spinning cylinders on their sides generally leads to fairly stable steady-state motions. However, as the aspect ratio gets closer to $\tilde{\ell} = \sqrt{3}/2$, the cylinders become susceptible to instabilities that make it more difficult to obtain data. In addition, cylinders can also be spun on their ends, but in this case, they need to be spun by hand, which makes the process more challenging (it takes practice to learn to spin a cylinder with its center of mass essentially at rest). While the motions for small θ are quite stable, it takes a lot of patience to obtain steady-state motions for larger θ (near the band of instability in Fig. 4).

The cylinder data are shown in Fig. 6 for aspect ratios $\tilde{\ell} = 2.5$ (squares), 1.5 (circles), and 1.0 (triangles), along with the predictions from Eq. (15). The solid (dashed) portions of the curves represent stable (unstable) motion, as described in the Appendix. The upper curves correspond to cylinders spinning on their sides, and the lower curves correspond to cylinders spinning on their ends. As can be seen, the experimental data agree reasonably well with the predictions in both regimes.

The procedure for obtaining spinning disk data is similar to that for cylinders. To obtain data for disks spinning on one face (lower left portion of Fig. 4), we spin the disks up to a high rotation rate and then make a number of short videos as the energy decreases. In this case, we found that it was more difficult to obtain steady-state motions for smaller-aspect-ratio disks. The motion was quite stable initially, but as the rotation rate slows, the small-aspect-ratio disks would generally become unstable to oscillatory motions. After some time, the rotation rate would begin to increase and the motion would become more stable. To obtain data for disks spinning on their edges, the disks were spun by hand. Again, care and patience was necessary to obtain appropriate steady-state motions.[37] Figure 7 shows experimental data for disks with aspect ratios $\tilde{\ell} = 0.75$ (squares) and 0.375 (circles). Once again, we obtain reasonable agreement with

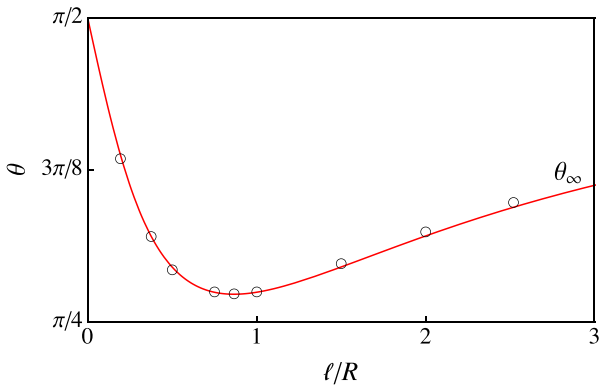

Fig. 5. Experimental results for steady-state motions of cylinders and disks at very high rotation rates ($\gtrsim 100$ Hz). The curve is given by the prediction from Eq. (15), namely, $\theta_\infty = \arctan(I_1/I_3\tilde{\ell})$.

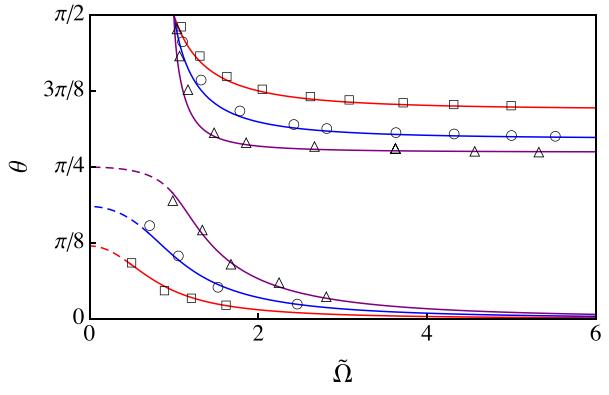

Fig. 6. Experimental results for steady-state motions of spinning cylinders with aspect ratios $\tilde{\ell} = 2.5$ (squares), 1.5 (circles), and 1.0 (triangles). The predictions are plotted using Eq. (15), showing both stable (solid) and unstable (dashed) solutions (see Appendix).

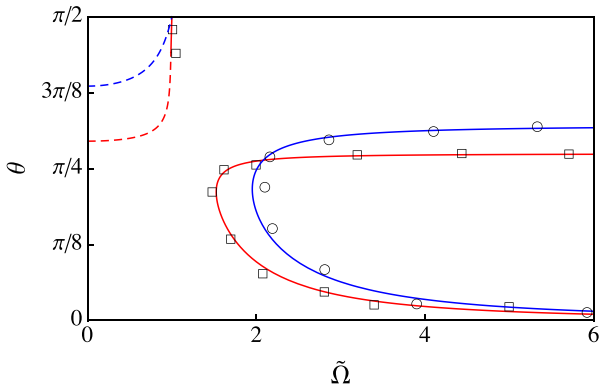

Fig. 7. Experimental results for steady-state motions of spinning disks with aspect ratios $\tilde{\ell} = 0.75$ (squares) and 0.375 (circles). The predictions are plotted using Eq. (15), showing both stable (solid) and unstable (dashed) solutions.

the predictions (the fact that the "middle" points show more discrepancy with the predictions is due to the difficulties we had in obtaining steady-state motions for these angles).

Finally, we discuss the special case $\tilde{\ell} = \sqrt{3}/2$, which occurs when $I_1 = I_3$. For this aspect ratio, Eq. (15) gives solutions $\theta = \arcsin(1/\tilde{\Omega}^2)$, for $\theta \neq \arctan(2/\sqrt{3})$. Although there is no forbidden region for this aspect ratio, Fig. 4 shows that there is a band of unstable (steady-state) solutions just above the point where the curves θ_0 and θ_∞ intersect. In addition, the angle $\theta = \arctan(2/\sqrt{3})$ occurs precisely where θ_∞ and θ_0 cross, suggesting that multiple rotation rates are possible at this angle. At first glance, it might seem odd to have two different rotation rates corresponding to one angle, but given that $\theta = \arctan(R/\ell)$ is the balancing angle, perhaps this is not so strange after all. In fact, with reference to the curves in Figs. 6 and 7 (and in particular, the curves with $\tilde{\ell} \to \sqrt{3}/2$ that are not shown in the figure), it would appear that *any* rotation rate will correspond to a steady-state solution at this angle. In other words, the value $\theta = \arctan(2/\sqrt{3})$ corresponds to a set of solutions for all $\tilde{\Omega}$, with $\tilde{\Omega} < (7/4)^{1/4}$ being unstable and $\tilde{\Omega} > (7/4)^{1/4}$ being stable (see Fig. 8).

It is worth mentioning that the experimental data in Fig. 8 were a bit tricky to obtain, especially near the unstable portions of the curves. In fact, although the data fit the predictions fairly well overall, one can see that the data seem less reliable near the point where the curves intersect. This is due, primarily, to the motion being very unstable to oscillatory-type behaviors in this regime.

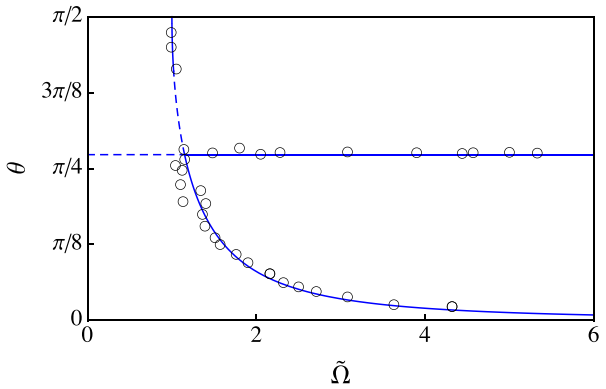

Fig. 8. Experimental results for steady-state motions of a spinning cylinder with the critical aspect ratio $\tilde{\ell} = \sqrt{3}/2$. The prediction is made up of two parts: (i) $\theta = \arcsin(1/\tilde{\Omega}^2)$, from Eq. (15), for $\theta \neq \arctan(\sqrt{3}/2)$, with stable (solid) and unstable (dashed) solutions as determined in the Appendix; and (ii) the horizontal line $\theta = \arctan(\sqrt{3}/2)$, with stability and instability determined by the limiting behavior of disks and cylinders for $\tilde{\ell} \to \sqrt{3}/2$.

V. CONCLUSION

A spinning cylinder represents a fascinating rigid-body motion that can be effective at engaging students and helping them get practice with topics such as vector analysis, principal axes, the inertia tensor, rotation matrices, and stable versus unstable motions. The disappearing-symbol phenomenon is a captivating mystery that will naturally draw students in and motivate their study. Although the general motion of a spinning cylinder is quite complex, making a few reasonable assumptions and analyzing the steady-state motion renders the problem tractable for students as early as their sophomore year.

One nice feature of this system is that while the steady-state motion seems quite simple, there is still a tremendous amount of interesting physics to uncover. The mystery of the disappearing symbols, while fascinating in and of itself, is only the beginning. Deriving the equation of motion and analyzing what it tells us are ways for students to experience what it is like to solve a new problem for the first time. In this sense, this problem works very well as an extended project in which students work as independent researchers (with an advisor) to uncover all that the system has to offer, both theoretically and experimentally. While the stability analysis may be a bit challenging for students to tackle on their own, the concepts are not difficult to understand, so with appropriate guidance they can make progress here as well.

Much of the material presented here has been successfully used in a sophomore-level mathematical methods course and also in a junior-level classical mechanics course. Portions of this material—for example, the disappearing-symbol phenomenon and its resolution as a case of velocity addition—could even be used in an introductory course. The analysis discussed here represents an example of how a simple real-world problem can be used to captivate and motivate students taking physics, whether at the introductory or advanced level. Incorporating such problems into courses seems to be a surefire way to create excitement and improve student learning.

ACKNOWLEDGMENTS

D.P.J. acknowledges the students in his Physics 282 courses over the past several years for their patience and feedback as portions of this material were developed. (The co-authors of this paper are former 282 students who took part in an independent-study project to explore this system in more detail.) The authors thank Jonathan Barrick for supplying us with a steady stream of cylinders made from different materials and with different aspect ratios. The authors also acknowledge Lars English and Brett Pearson for thoughtful conversations and helpful suggestions.

APPENDIX: STABILITY ANALYSIS

We use an energy approach to study the stability of this system, keeping the variables completely general initially.[38] The kinetic energy is then

$$T = \frac{1}{2} I_1 \dot{\phi}^2 \sin^2\theta + \frac{1}{2} I_2 \dot{\theta}^2 + \frac{1}{2} I_3 \left(\dot{\psi} + \dot{\phi}\cos\theta\right)^2, \qquad \text{(A1)}$$

while the potential energy is

$$V = Mg(\ell \cos\theta + R \sin\theta). \qquad \text{(A2)}$$

Forming the Lagrangian $\mathcal{L} = T - V$ and determining the Lagrange equations, one finds that the variables ϕ and ψ are ignorable so that the generalized momenta p_ϕ and p_ψ are constant. These generalized momenta turn out to be the components of angular momenta along the vertical axis (L_z) and the symmetry axis (L_3), respectively. [Note that at this point, one can use the system constraints in the θ equation to arrive at the correct equation of motion given by Eq. (15)].

We next write the energy $E = T + V$ and substitute for $\dot{\phi}$ and $\dot{\psi}$ in terms of the constants L_z and L_3, resulting in an equation of the form

$$E(\theta) = \frac{1}{2} I_2 \dot{\theta}^2 + U_{\text{eff}}(\theta), \qquad \text{(A3)}$$

where $U_{\text{eff}}(\theta)$ is an effective potential energy for what is now a one-dimensional problem. This equation is generally used to demonstrate nutation in a spinning top, as θ oscillates back and forth in a potential well. For our purposes, we assume that the energy of the system dissipates rather quickly so that a spinning cylinder ends up at the bottom of the well, which represents steady-state motion. As such, one can set $dU_{\text{eff}}/d\theta = 0$ to determine the critical points for this system. Replacing L_z and L_3 and using the system constraints will then lead to Eq. (15), which can thus be seen as an equation for the critical points of the system.

To determine whether we are dealing with energy minima or energy maxima, we take the second derivative $d^2U_{\text{eff}}/d\theta^2$, evaluate it at the critical points, and check to see whether they are positive (energy minimum) or negative (energy maximum). While the determination of the critical points, Eq. (15), can be carried out analytically, the determination of where the second-derivative is positive or negative must be handled numerically.

[a]Electronic address: jacksond@dickinson.edu

[1]A. D. Fokker, "The rising top, experimental evidence and theory," Physica **8**, 591–596 (1941).

[2]Several aspects of spinning tops, including the behavior of a tippe top, is discussed in R. Cross, "The rise and fall of spinning tops," Am. J. Phys. **81**, 280–289 (2013).

[3]The basic mechanism responsible for the behavior of a rattleback can be found in W. Case and S. Jalal, "The rattleback revisited," Am. J. Phys. **82**, 654–658 (2014).

[4]According to Ref. 3, the rattleback was investigated as far back as 1896 by G. T. Walker, "On a dynamical top," Q. J. Pure Appl. Math. **28**, 175–184 (1896), but the toy was popularized in the 1970s by J. Walker, "The mysterious 'rattleback': A stone that spins in one direction and then reverses," Sci. Am. **241**, 172–184 (1979).

[5]W. L. Andersen and Steven Werner, "The dynamics of hurricane balls," Eur. J. Phys. **36**, 055013-1–7 (2015).

[6]D. P. Jackson, D. Mertens, and B. J. Pearson, "Hurricane Balls: A rigid-body-motion project for undergraduates," Am. J. Phys. **83**, 959–968 (2015).

[7]K. C. Mamola, "A rotational dynamics demonstration," Phys. Teach. **32**, 216–219 (1994).

[8]A. E. Sikkema, S. D. Steenwyk, and J. W. Zwart, "Spinning tubes: An authentic research experience in a three-hour laboratory," Am. J. Phys. **78**, 467–470 (2010).

[9]L. A. Whitehead and F. L. Curzon, "Spinning objects on horizontal planes," Am. J. Phys. **51**, 449–451 (1983).

[10]J. Walker, "The Amateur Scientist: Delights of the 'wobbler,' a coin or cylinder that precesses as it spins," Sci. Am. **247**, 184–193 (1982).

[11]The front page of the Veritasium YouTube channel is <https://www.YouTube.com/user/1veritasium> and the specific link to the spinning cylinder trick is <https://www.YouTube.com/watch?v=wQTVcaA3PQw>. The number of views for this particular video was 3 832 871 as of July 4, 2018.

[12]M. R. A. Shegelski, I. Kellett, H. Friesen, and C. Lind, "Motion of a circular cylinder on a smooth surface," Can. J. Phys. **87**, 607–614 (2009).

[13]Indeed, while the rolling-disk phenomenon is "familiar and often interesting," its study was regarded mainly as a "point of honour…even if the solution should prove to be impracticable, or difficult of interpretation." H. Lamb, *Higher Mechanics* (Cambridge U. P., Cambridge, 1920), pp. 158–159.

[14]M. G. Olsen, "Coin spinning on a table," Am. J. Phys. **40**, 1543–1545 (1972).

[15]W. L. Anderson, "Noncalculus treatment of steady-state rolling of a thin disk on a horizontal surface," Phys. Teach. **45**, 430–433 (2007).

[16]A very readable treatment of the rolling disk problem is provided by A. K. McDonald and K. T. McDonald, "The rolling motion of a disk on a horizontal plane," preprint arXiv:physics/0008227v3 (2002).

[17]*Euler's disk* was developed by Joseph Bendik after mistakenly being sent a box of 12 polishing chucks and becoming obsessed with spolling (spinning/rolling) disks. Additional information is available at <http://eulers-disk.com/>.

[18]*Euler's Disk* even found its way onto the popular television show *The Big Bang Theory* (season 10, episode 16).

[19]H. K. Moffat, "Euler's disk and its finite-time singularity," Nature **404**, 833–834 (2000).

[20]See, for example, the comment by G. van den Engh, P. Nelson, and J. Roach, "Numismatic gyrations," Nature **408**, 540, (2000), along with Moffat's response.

[21]See, e.g., D. Ma, C. Liu, Z. Zhao, and H. Zhang, "Rolling friction and energy dissipation in a spinning disc," Proc. R. Soc. A **470**, 20140191-1–22 (2014), and references therein.

[22]In addition to playing around in class, the hope is that students will show it to their friends and continue to think about what makes the Xs (or Os) disappear.

[23]See supplementary material at https://doi.org/10.1119/1.5086391 for some slow-motion videos of spinning cylinders and disks.

[24]Beginning students might suggest using the equation $\boldsymbol{\Gamma}_{\text{net}} = I\boldsymbol{\alpha}$, where I is the object's moment of inertia and $\boldsymbol{\alpha}$ is the angular acceleration vector. Unfortunately, this equation is not valid in this situation. It may be worth reminding students that the equation $\mathbf{F}_{\text{net}} = m\mathbf{a}$ is not always valid either (e.g., when the system has a changing mass) and in such cases we must appeal to the more general form of Newton's second law: $\mathbf{F}_{\text{net}} = d\mathbf{p}/dt$, where $\mathbf{p}$ is the momentum of the system. Likewise, the equation $\boldsymbol{\Gamma}_{\text{net}} = I\boldsymbol{\alpha}$ is not generally valid (e.g., when the angular velocity is not aligned with one of the principal axes), so we must appeal to the more general form given in Eq. (3).

[25]Comparing Fig. 4 of Ref. 6 to Fig. 2 here shows a lot of similarities. Indeed, the analysis is similar in some ways; however, the variable aspect ratio for a cylinder adds a new layer of complexity to the problem and leads to a lot of interesting physics not found with *Hurricane Balls*.

[26]The symbol on the stationary end is quite clear while the symbol on the moving end is a completely blurred out.

[27]A very nice photograph of a spinning cylinder that uses LEDs in the ends of the cylinder can be found in E. Bormashenko and A. Kazachkov, "Rotating and rolling rigid bodies and the 'hairy ball' theorem," Am. J. Phys. **85**, 447–453 (2017).

[28]Another way of figuring things out is by noting that for an object that is rolling without slipping, the point of contact is instantaneously at rest. Knowing that both the center of mass C and the point of contact P are both at rest defines the instantaneous axis of rotation. All points on the instantaneous axis of rotation—including the uppermost point—are (instantaneously) at rest.

[29]Generally speaking, it is much more difficult to calculate the inertia tensor analytically without using a set of principal axes. For example, trying to calculate the components of the inertia tensor in the (x, y, z) coordinate system in Fig. 2 would present a significant challenge.

[30]The Lagrangian approach can be used, but it must be approached with care (see Appendix).

[31]In analogy with spheroids, we might instead refer to prolate and oblate cylinders instead of cylinders and disks.

[32]Although we analyzed the situation of a cylinder rolling on its side, Eq. (15) is also valid for a cylinder rolling on its end. In this sense, we also get the steady-state solutions to *Euler's Disk* for "free."

[33]Point D represents an energy maximum on the vertical line $\tilde{\ell} = 2.5$. In fact, there is a curve of such maxima (forming a "ridge" in the energy landscape) that lies below and follows the boundary (dashed curve) between stable and unstable solutions, osculating this boundary at the point where θ_∞ and θ_0 intersect.

[34]Interestingly, while the rotation rate $\boldsymbol{\Omega} \to \infty$ as $\theta \to 0$, the face of the coin will actually become stationary. This can be understood by noting that rotations about the vertical axis and rotations about the symmetry axis cancel out as $\theta \to 0$. From Eq. (6), we see that $\dot{\psi} \to -\dot{\phi}$ while $\hat{\mathbf{e}}_3 \to \hat{\mathbf{e}}_z$ (see Fig. 2). The end result is that $\boldsymbol{\omega}$ [see Eq. (4)] (and $\mathbf{L}$) goes to zero as $\theta \to 0$.

[35]We did our best to make sure the experimental results were obtained when the center of mass was at rest and θ was constant, but some aspect ratios were very susceptible to instabilities at specific rotation rates. Thus, while our experimental data are obtained with good precision (reasonably small error bars), it is likely that some of our spinning cylinders (and disks) were not true steady-state motions (our patience was limited).

[36]*Tracker* is an open source video-analysis and modeling program that is freely available online at <http://physlets.org/tracker/> or on ComPADRE at <https://www.compadre.org/osp/items/detail.cfm?ID=7365>.

[37]In Fig. 7, notice that the upper (disk on its side) $\tilde{\ell} = 0.75$ curve is almost vertical near $\theta = \pi/2$. In fact, the angular speeds for some disks having aspect ratios near $\tilde{\ell} = \sqrt{3}/2$ are predicted to first increase slightly above $\tilde{\Omega} = 1$ before decreasing to $\tilde{\Omega} = 0$.

[38]See, for example, J. R. Taylor, *Classical Mechanics* (University Science Books, Sausalito, 2005), pp. 403–407.

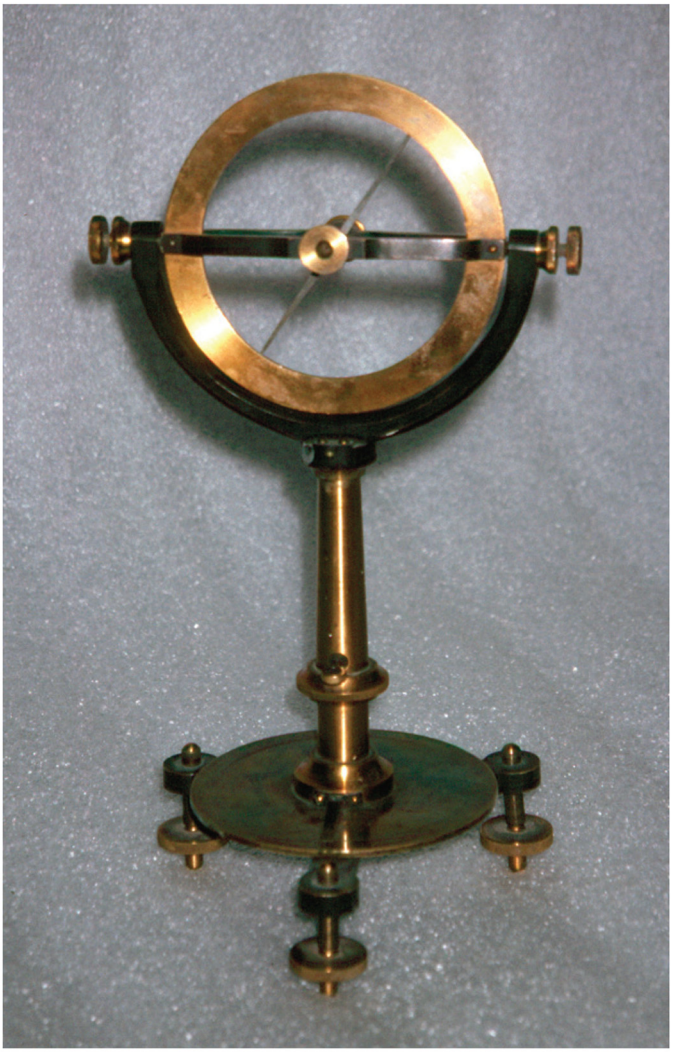

Dip Needle

The ordinary compass is used to indicate the direction of the horizontal component of the magnetic field of the earth. If it is turned up on edge it will show that angle that the magnetic field makes with the vertical. The needle must be accurately balanced so that only magnetic torque is exerted on it. This example was made by Queen of Philadelphia during the latter years of the 19th century when the company was the largest provider of apparatus for physical experimentation in the United States. I photographed it in the demonstration room of the University of Utah during a break of the 2005 summer meeting of the American Association of Physics Teachers. (Notes and photograph by Thomas B. Greenslade, Jr., Kenyon College)